HiSST: 3rd International Conference on
High-Speed Vehicle Science Technology
14 -19 April 2024, Busan, Korea

Design and Analysis of Double Design Point Inward-turning Inlet with Osculating Method

Zejun Cai[1], Xiaogang Zheng[2], Waner Hu[3], Zhancang Hu[4], Chengxiang Zhu[5], Yancheng You[6]

Abstract

The inward-turning hypersonic inlet is pivotal for ensuring optimal incoming flow to the engine, particularly across wide-speed range. However, conventional single design point methods often neglect performance variations across different speeds. To tackle this, a novel Double Design Point (DDP) osculating inward-turning inlet design method is proposed. This method considers mass flow capture under varied flow conditions, offering a comprehensive solution for hypersonic inlet design challenges. High/low Mach design points and mass flow rate are key parameters in DDP design, with the lip streamline crucial for determining mass flow at low Mach points. By integrating these factors, the DDP method effectively addresses hypersonic inlet design challenges. Results indicate that, the DDP basic flow field has excellent agreement with CFD data with less than 1% error. Notably, in osculating inward-turning inlet design, DDP aligns well with the high Mach design point, yielding a mass flow rate of 0.99. However, the influence of 3D effects diminishes mass flow capture at the low Mach design point, the mass flow rate is 0.69 with a design value at 0.80. The main mismatch occurs at the stream trace with a value at 0.53, while the osculating region has a much higher capture ability at 0.75.

Keywords: *Hypersonic inlet, Inward-turning inlet, Wide-speed range, Osculating design*

Nomenclature

φ –mass flow rate
π – pressure ratio
θ – extend angle

1. Introduction

The hypersonic inlet is a critical component for ensuring efficient and wide-ranging flight of air-breathing aircraft. Its primary purpose is to provide compressed air to meet the engine's requirements throughout the flight envelope, including acceleration, deceleration, and cruise phases [1]. Among the different inlet configurations, the inward-turning inlet has attracted significant attention in recent years due to its superior performance in compression, flow capture, and windward area [2]. This configuration has been embraced by several developments in hypersonic aircraft, including the SR-72 [3], HAWC [4], and Boeing's hypersonic aircraft [5], all of which utilize the inward-turning inlet design to achieve a wide-speed range flight.

Since the inward-turning inlet is essentially a streamline-traced tube in the basic flow field [6]., the design of the basic flow field has become a crucial factor in achieving the optimal performance of the hypersonic inlet. The design of the basic flow field can be broadly classified into two categories: forward design [7-10] and inverse design [11-15]. The forward design method involves using the wall boundary as the design input, and it has traditionally relied on iterative optimization for evaluation during scheme design.

[1] *Xiamen University, Xiamen Fujian, caizejun@stu.xmu.edu.cn*
[2] *Xiamen University, Xiamen Fujian, xiaogangzheng@xmu.edu.cn*
[3] *Xiamen University, Xiamen Fujian, 35020231151582@stu.xmu.edu.cn*
[4] *Xiamen University, Xiamen Fujian, 35020200156007@stu.xmu.edu.cn*
[5] *Xiamen University, Xiamen Fujian, chengxiang.zhu@xmu.edu.cn*
[6] *Xiamen University, Xiamen Fujian, yancheng.you@xmu.edu.cn*

Ma Yue [16] employed dynamic multi-objective optimization to improve the total pressure recovery and drag at design point using Kriging-based modeling and computational fluid dynamics. Damm [17], on the other hand, utilized a discrete adjoint method with RANS analysis to optimize the inward-turning inlet configuration. Despite achieving improved performance, this method consumes a substantial amount of computational resources, and the optimization result yields a reflected shock removal flow field. In contrast, the inverse design method uses the outlet characteristics as input to construct the flow field, resulting in a higher design efficiency. For instance, Qiao [18] applied the method of characteristic (MOC) to inverse design the basic flow field without a reflected shock, a similar approach to Damm's work [17], but with much lower computational resource consumption. Therefore, it can be concluded that if a flow field structure with the required performance can be constructed, the efficiency and effectiveness of constructing such a flow characteristic through the inverse design method will be much better than that of the forward design method.

The traditional forward and inverse design methods of inward-turning inlets are facing new challenges due to the increasing demands for wide-speed domain performance [19,20]. These challenges include the ability to start at low Mach conditions [3,21], unpredictable performance deterioration during off-design conditions [22-24], and variable geometry capability. However, both of these methods are designed based on a single design point, which renders the off-design performance unpredictable. To meet the wide-speed domain demand, it usually requires iterative optimization at both design and off-design points as to a forward design process [25]. Shuvayan [26] applied multi-objective design optimization method in an improved Busemann-based inlet. The optimization result exhibited better performance than the original design at the design point, and it also met the temperature demand at the off-design point. As to an inverse design method, data-driven wide-speed domain flow field inverse design methods are the only ones available due to the absence of a direct correlation between wide-domain flow structure and performance. Researchers such as Fujio and Ogawa [27-29] have utilized global optimization methods which rely on flow field data across a broad spectrum of conditions to develop a data-driven wide-speed range flow field inverse design approach. As compared to the previous MOC inverse design method, this new approach heavily relies on the flow field in the database to generate the design. Therefore, if the design requirements exceed the boundaries of the database, the effectiveness of the obtained flow field may not be guaranteed.

Previous research has developed a double design point (DDP) design method that considers a wide range of performance requirements. This method utilizes the high and low Mach design point mass flow rate demand as the primary design input. However, the constraint on the entry shape limits the design freedom. To address this limitation, this paper proposes the application of the osculating method to enhance design freedom and extend the DDP method to the entry shape unlimited inlet design.

2. Design method of double design point osculating inward-turning inlet

2.1. Double design point flow field design

The osculating DDP inward-turning inlet design method is based on the application of the DDP basic flow field. It employs an axisymmetric flow field, where the high and low Mach design point mass flow rates serve as the design parameters. At the high Mach design point, full flow capture is achieved. Fig. 1 illustrates the composition of the DDP basic flow field, with dashed lines representing the curved shock curve, solid lines in different colors representing different sections of the wall boundary, and light-yellow columns representing the centerbody of the high and low Mach design points. In an axisymmetric flow field, the flow capture ability (φ) can be expressed as the ratio of the area of the captured flow tube's concentric circles to the area of the inlet's concentric circles, as shown in Eq.1. The inner circle of the captured flow tube is formed by a streamline passing through the lip point (lip streamline) in Fig. 1. Consequently, the key aspect of the DDP flow field is to ensure that the lip streamline begins at a specific height and reaches the lip point under low Mach design point conditions while the high Mach incident shock reaches the lip point.

Considering this, the basic flow field is divided into three parts. The first part is determined by the low Mach incident shock instead of the high Mach incident shock, and it corresponds to the area generated by wall boundary I. The second part is designed through a step-by-step forward design process, with the aim of geometrically intersecting the high Mach incident shock and the low Mach lip streamline at a specified height of the lip point. This part corresponds to the area generated by wall boundary II.

The third part is determined by the high Mach reflected shock, which also causes curvature in the centerbody, and it corresponds to the area on wall boundary III.

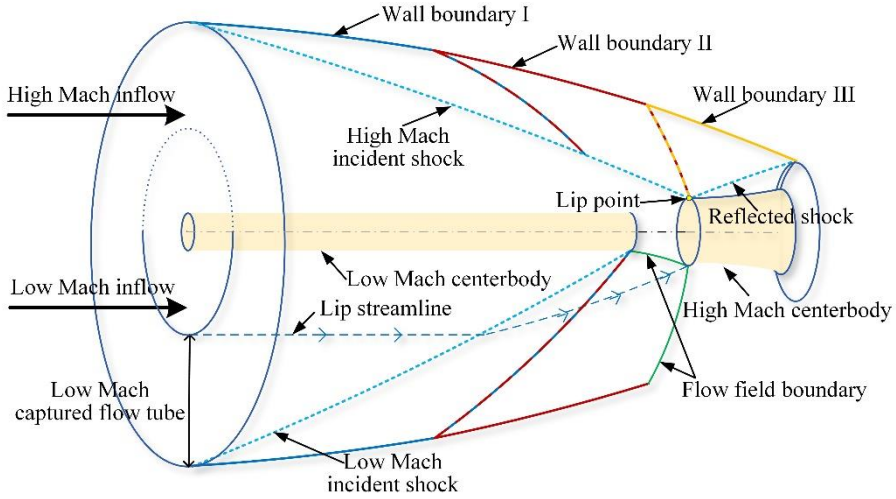

Fig 1. Deconstruction of double design point basic flow field

$$\varphi = \frac{y_{begin}^2 - y_{lip}^2}{y_{begin}^2 - h_{high}^2} \tag{1}$$

The osculating DDP inward-turning inlet design method is based on the application of the DDP basic flow field. It employs an axisymmetric flow field, where the high and low Mach design point mass flow rates serve as the design parameters. At the high Mach design point, full flow capture is achieved. Fig. 1 illustrates the composition of the DDP basic flow field, with dashed lines representing the curved shock curve, solid lines in different colors representing different sections of the wall boundary, and light-yellow columns representing the centerbody of the high and low Mach design points. In an axisymmetric flow field, the flow capture ability (φ) can be expressed as the ratio of the area of the captured flow tube's concentric circles to the area of the inlet's concentric circles, as shown in Eq.1. The inner circle of the captured flow tube is formed by a streamline passing through the lip point (lip streamline) in Fig. 1. Consequently, the key aspect of the DDP flow field is to ensure that the lip streamline begins at a specific height and reaches the lip point under low Mach design point conditions while the high Mach incident shock reaches the lip point.

Considering this, the basic flow field is divided into three parts. The first part is determined by the low Mach incident shock instead of the high Mach incident shock, and it corresponds to the area generated by wall boundary I. The second part is designed through a step-by-step forward design process, with the aim of geometrically intersecting the high Mach incident shock and the low Mach lip streamline at a specified height of the lip point. This part corresponds to the area generated by wall boundary II. The third part is determined by the high Mach reflected shock, which also causes curvature in the centerbody, and it corresponds to the area on wall boundary III.

2.2. Osculating design in double design point method

In the context of inward-turning inlet design and the utilization of the DDP basic flow field, maintaining a consistent relative height relationship between the lip streamline, lip point, and leading edge of the inlet is crucial. This necessity dictates a fan-shaped entry shape for the inlet. To augment design flexibility, the osculating method is employed in this paper. Fig. 2 illustrates the osculating design method for inward-turning inlets. In Fig. 2(a), the red zone represents the osculating region of the entry shape, where the osculating design method is applied, while the blue zone represents the regular stream trace region. The corresponding inlet surface of these regions is depicted in the same color. The outermost circle represents the shock wave profile curve (SWPC), with dashed lines at symmetry denoting the incident shock and reflected shock of the local DDP basic flow field. Fig. 2(b) presents the theoretical characteristics of the inlet at the low Mach design point. The red zone symbolizes the mass

flow captured by the osculating region, while the grey zone represents the overflow. The green arrow lines denote the lip streamlines, which collectively form the lip stream surface illustrated in yellow.

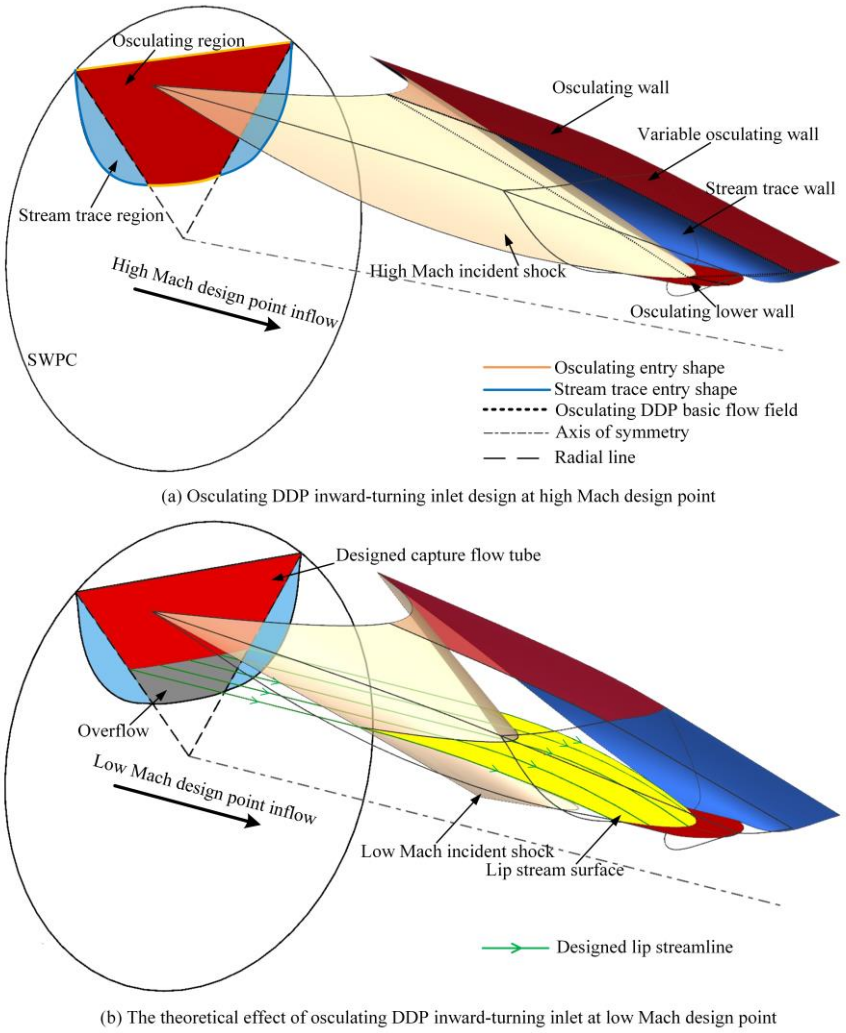

Fig 2. Osculating design method in double design point inward-turning inlet

Given the limited number of feasible solutions for the lower surface to meet the mass flow rate requirement while maintaining consistency with the upper surface, conducting DDP design across all osculating planes is impractical. To ensure geometric continuity of the inlet, a portion of the surface will adopt a streamline tracing approach. This entails dividing the corresponding inlet shape into two regions: the osculating region and the stream trace region. In the osculating region, the upper entry shape serves as the design input, with the lower entry shape determined iteratively during the osculating design process. Conversely, for the stream trace region, a curve connecting the upper and lower osculating entry shapes is utilized as the stream trace entry shape. Both regions' inlet surfaces are fashioned using the high Mach design point DDP basic flow field. Within the osculating region, the upper and lower curves of the inlet surface are derived based on the local DDP basic flow field. The stream trace surface is generated from this local DDP basic flow field where the upper and lower boundary points of the osculating entry shape are. The mass flow rate in both regions would achieve 1, as the incident shock generated by the inlet effectively seals the inlet entrance. Concerning the low Mach design point mass flow capture characteristics, the mass flow rate is determined by a combination of the osculating and stream trace regions. In the osculating region, the mass flow rate is calculated as the ratio of the area of designed capture flow tube to the entire osculating region. This ratio is designed to align with the intended mass flow rate. However, the stream trace region lacks a predefined design value, potentially leading to a discrepancy between the inlet design and the DDP method.

With the osculating method now clarified, the subsequent text introduces the design approach for the local DDP basic flow field. In Fig. 3, the dashed line represents the parent basic flow field, with the high

Mach flow field depicted in red and the low Mach flow field shown in blue. The solid line portrays the local basic flow field. The lip streamlines of the parent and local flow fields are illustrated by yellow dashed and solid lines, respectively. Given the upper osculating entry shape, the upper wall boundaries I&II are derived from the parent high Mach design point flow field. Subsequently, the corresponding low Mach design point flow field can be obtained through the compute of low Mach flow field. The subsequent step involves pinpointing a streamline within this low Mach flow field and establishing it as the starting point for the local lower wall boundary by determining its intersection with the high Mach shock curve. Furthermore, the relationship between the starting point and the local lip streamline should adhere to Eq.1. Lateral to this process, the wall boundary III and the lower wall boundary can be reconstructed. The collection of upper and lower wall boundaries generated in this procedure constitutes the osculating inlet surface.

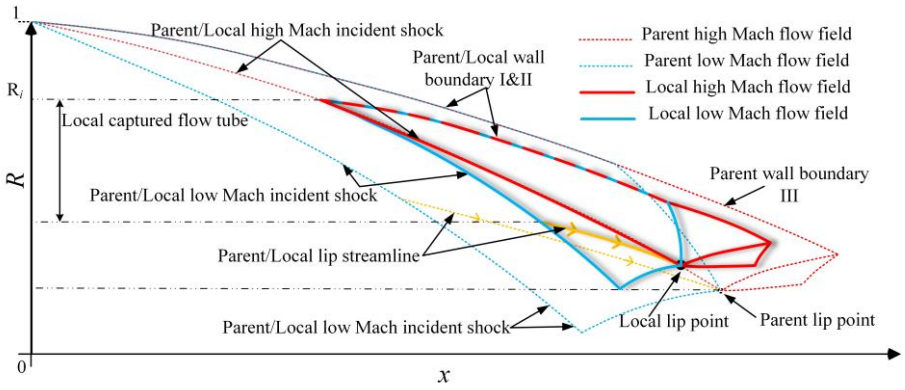

Fig 3. The design method of DDP basic flow field on local osculating plane

3. Numerical verification and analysis

3.1. Numerical methods and validation

The numerical method described in the previous section was employed in this study to simulate the experimental model presented in [30]. The cross-section of the model is shown in Fig. 4(a), and the inflow conditions are based on the reference in [30]. Fig. 4(b) compares the pressure distribution on the upper and lower walls between the experiment and simulation. It can be observed that both the numerical and experimental results exhibit close agreement in terms of the pressure distribution and overall trend. The above validation demonstrates the accuracy of the computational method used in this study, supporting the simulation-based investigation of the aerodynamic performance presented in this paper.

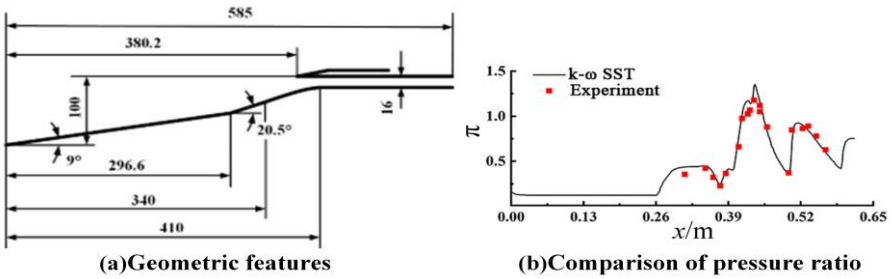

Fig 4. Numerical example verification of cases and comparison of wall pressure distribution

The present study solves the three-dimensional Reynolds-Averaged Navier-Stokes (RANS) equations based on density. The inviscid convective fluxes are computed using the second-order upwind Roe-FDS differencing scheme. The convergence criterion for the computational process is to reduce the residuals of the continuity equation, momentum equation, and energy equation by at least three orders of magnitude, while ensuring a stable mass flow rate at the outlet cross-section of the inlet duct. Air is assumed to be an ideal gas, with the specific heat capacity at constant pressure (C_P) modeled using a Piecewise-Polynomial fit. As shown in Fig. 5(a), the freestream face is defined as the pressure far-field boundary, while the outlets is considered pressure outlets. The wall boundaries are treated as adiabatic

with no-slip conditions, neglecting heat transfer. To meet the scale requirements of different design point Mach numbers, multiple sets of computational grids are employed in this study. Each grid set is refined near the wall surface, ensuring a y^+ value of no greater than 30. In order to accommodate the diverse flow conditions associated with different Mach numbers, several computational grid configurations are utilized.

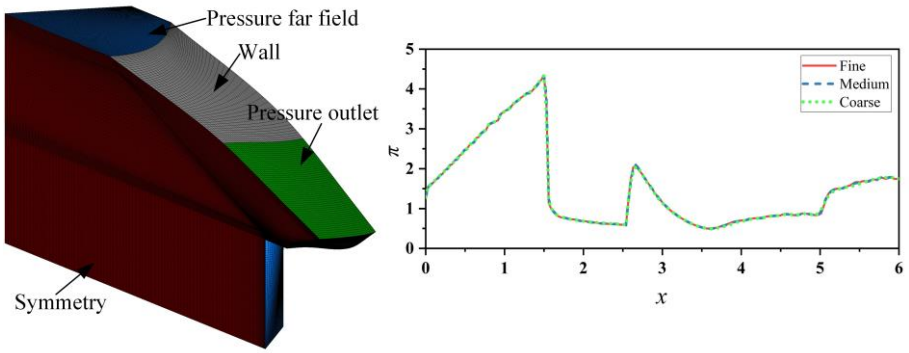

(a) Boundary conditions and mesh (b) Comparison of pressure ratio along the upper wall

Fig 5. Grid sensitivity analysis

To ensure the reliability of the computational results, a grid independence verification was conducted for the Ma3 side fender B case. This involved a comparison of coarse, medium, and fine grids, as depicted in Fig. 5(b). It portrays the pressure ratio along the intersection line between the upper wall and the symmetry plane. The vertical axis represents the pressure ratio of wall curve at symmetry plane, while the horizontal axis corresponds to the x-direction coordinate. Notably, the pressure ratio demonstrates a consistent trend across various mesh sizes, with all curves fitting well. Consequently, this article adopts a medium grid size for the numerical simulation. The grid resolution for other computational conditions was adjusted accordingly.

3.2. Numerical verification of DDP basic flow field

The basic flow field considered in this article is a typical steady, isentropic, and rotational supersonic flow field. To evaluate the effectiveness of the DDP design method, a CFD simulation is performed. The wall boundary derived from the method is incorporated into the simulation under the same high/low inflow conditions. The CFD zone concludes at the last C_- and C_+ passing through the lip point obtained through the MOC calculation.

Fig. 6 presents the characteristics of the DDP basic flow field computed by both MOC and CFD. In Fig. 6(a)(b), the CFD flow field is shown in contour, while the MOC result is represented by the red dashed line. The black arrow line indicates the lip streamline obtained from CFD (LS_{CFD}), while the blue hollow dot lines represent the lip streamline obtained from the MOC method (LS_{MOC}). Fig. 6(c) compares the shape and pressure ratio of the lip streamline. The scatter plots in blue and green represent the y-value and pressure ratio computed by MOC, respectively. The purple and brown lines correspond to the corresponding CFD results.

In Fig. 6(a), it can be observed that the incident shock reaches the lip point, and the reflected shock also reaches the upper wall boundary at the endpoint. This signifies that the high Mach design successfully captures the required mass flow rate, and the isoline of the MOC aligns closely with the CFD isoline. Similarly, for the low Mach design point, the two lip streamlines nearly coincide, and the contour lines exhibit a close match as well. The lip streamline initiates at a specified y-value, corresponding to φ=0.7, and extends to the lip point, which has a given y-value of 0.3 in this case. The average difference in pressure ratio is approximately 0.99%, indicating a strong alignment between the DDP basic flow field design method and the desired pressure conditions. Additionally, the average y-value difference is approximately 0.40%, further affirming the efficacy of the DDP method in achieving the intended flow characteristics. Overall, these observations highlight the effectiveness of the DDP basic flow field design method in achieving desired flow properties and support its application in practical design scenarios.

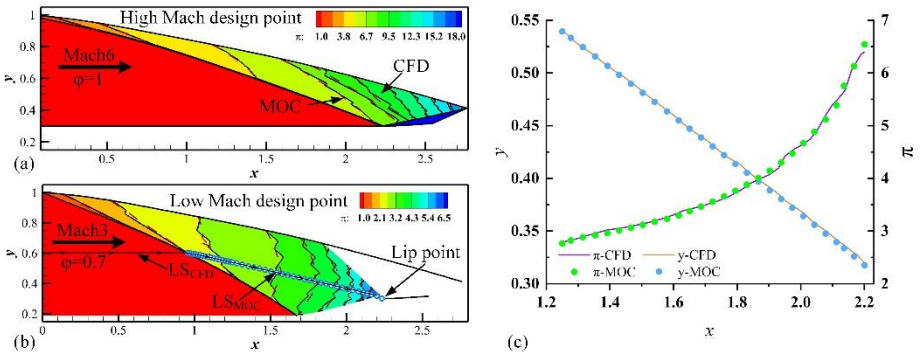

Fig 6. Verification of double design point method

3.3. Analysis of DDP osculating inward-turning inlet

The high Mach design point characteristics of the osculating inward-turning inlet are illustrated in Fig. 7. In Fig. 7(a), the alignment of the high Mach incident shock with the DDP basic flow field shock surface highlights the efficiency of the osculating design method, with the high Mach mass flow rate reaching 0.99. Moving to Fig. 7(b), the contour depicts the flow field of the inlet at the symmetric plane. The isolines in black represent the pressure ratio obtained from 3D CFD results, while the isolines in blue correspond to the pressure ratio of the local osculating DDP basic flow field. The comparison reveals that the pressure ratio distribution characteristics align well with the basic flow field. The incident shock curve matches the basic flow field, and the reflected shock curve near the lower side also exhibits a favorable correlation. Notably, the forward lean of the intersection between the upper wall and reflected shock is attributed to the internal contraction characteristic of the inlet. Despite this, the design method of the local DDP basic flow field is deemed effective, considering that the internal contraction characteristic is an inherent and advantageous feature of the inward-turning inlet.

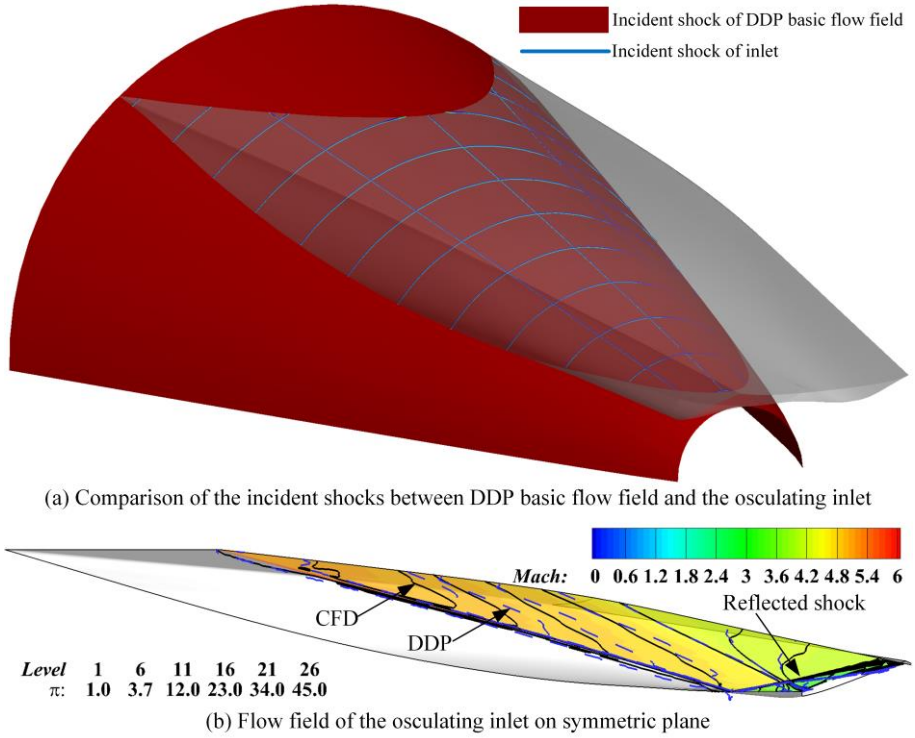

Fig 7. High Mach design point flow characteristics (Mach6)

The low Mach design point characteristics of the osculating inward-turning inlet are illustrated in Fig. 8. In Fig. 8(a), the mass flow capture characteristics of the inlet at the low Mach design point are depicted. The black line represents streamlines passing through the leading edge of the inlet, while the blue surface signifies the low Mach incident shock. The grey plane illustrates the entry shape of the inlet, and the red area denotes the captured mass flow area in the far field. In the top right corner, the impact of 3D effect on mass flow rate is presented. The red shaded area corresponds to the region

designed by regular stream trace, with the angle denoted as θ_2, while the region designed by the osculating DDP method is labeled as θ_1. The purple area represents the difference between the theoretical mass flow captured area and the actual captured area in the osculating region. Moving on to Fig. 8(b), the contour depicts the flow field of the inlet, with the black isoline representing the Mach distribution of the local osculating DDP basic flow field. The black dotted line signifies the lip streamline of the basic flow field (LS_{2D}), the purple dotted line represents the designed lip streamline in the DDP process (LS_{DDP}), the red arrow line corresponds to the lip streamline of the inlet (LS_{inlet}), and the green arrow line represents the streamline of the inlet passing through the leading point, aligning with both LS_{DDP} and LS2D (LS'_{inlet}).

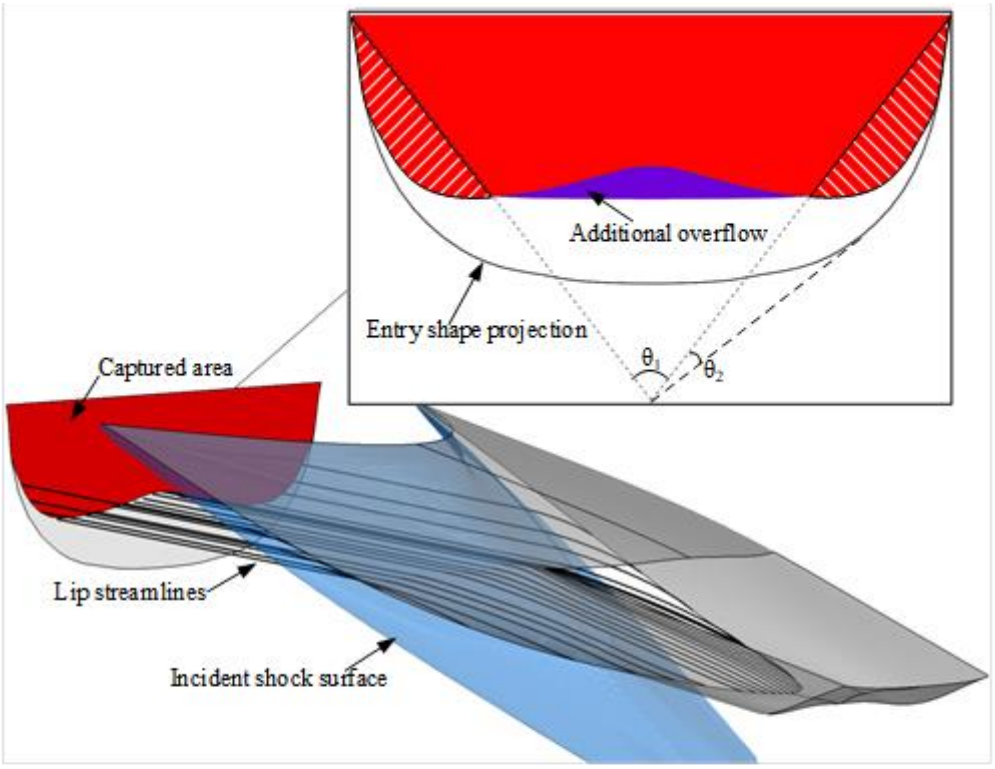

Fig 8. Low Mach design point flow characteristics (Mach3)

The incident shock remains unattached to the leading edge of the inlet, and the flow tube passing through the entry shape projection overflows from the lip side. Thereby, the mass flow captured by the inlet can be described as the flow tube enclosed by the lip streamlines on each osculating plane and the corresponding upper leading edge, represented by the red area in Fig. 8(a). According to this description, the mass flow rate at the low Mach design point is calculated to be 0.69, while the intended design value is 0.8. This discrepancy is attributed to the 3D effect. To assess the extent of the 3D effect, the mass flow rate of each region should be calculated separately. Recomputing the mass flow rate for each region reveals a value of 0.75 for the osculating region and only 0.53 for the stream trace region. The higher mass flow rate in the osculating region can be attributed to several factors: firstly, the upper and lower inlet surfaces of the osculating region are specifically designed to achieve a certain mass flow rate, whereas the stream trace region only considers the geometric closure requirement. Secondly,

the osculating region is located at the midpoint of the entry shape and indirectly experiences the 3D effect, while the stream trace region is directly influenced by the pressure gradient between the far flow and the high-pressure zone behind the incident shock.

In the absence of a theoretical mass flow rate for the stream trace region, the subsequent analysis hones in on the discrepancy within the osculating region. As depicted in Fig. 8(a), the deviation at the symmetry plane surpasses the boundary between the osculating region and the standard stream trace region, and the flow characteristics at the symmetry plane are illustrated in Fig. 8(b). The LS'_{inlet}, LS_{2D} and LS_{DDP} coincide with each other after passing through the incident shock. The alignment between LS_{2D} and LS_{DDP} persists up to the lip point, while LS'_{inlet} diverges outward due to the influence of the 3D effect. This 3D effect is induced by the vortex generated from the outer side of the leading edge, as identified in earlier research. On the other hand, the larger shock angle shifts the intersection point of the lip streamline and the incident shock to the upper side. Consequently, the LS_{inlet} is elevated compared to the other three streamlines. Despite this discrepancy, the DDP osculating design method can still be deemed effective, given the alignment between LS_{DDP} and LS'_{inlet}.

4. Conclusion

This paper introduces a methodology for the design of a double design point (DDP) osculating inward-turning inlet. The DDP approach takes into account the mass flow rate requirements at both high and low Mach design points. Leveraging the method of characteristics as the mathematical tool for designing the DDP basic flow field, the proposed approach is validated through a comparison with 2D numerical simulations. The results demonstrate a remarkable alignment with the design values for mass flow rate at both high and low Mach design points, with an error of less than 1%. Examining the 3D characteristics, the study observes significant alignment between the inlet and the DDP basic flow field at the high Mach design point, where the inlet achieves a mass flow rate of 0.99. However, at the low Mach design point, the 3D effects result in a reduction in mass flow capture ability, yielding a mass flow rate of 0.69 compared to the design value of 0.8. This deviation primarily occurs in the stream trace region, which records a value of 0.53, while the osculating region exhibits a value of 0.75, much closer to the design value.

References

1. Zuo F Y ,Mölder, Sannu.Hypersonic wavecatcher intakes and variable-geometry turbine based combined cycle engines[J].Progress in Aerospace Sciences, 2019, 106(APR.):108-144.DOI:10.1016/j.paerosci.2019.03.001.
2. You Y .An Overview of the Advantages and Concerns of Hypersonic Inward-turning Inlets[C]//Aiaa International Space Planes & Hypersonic Systems & Technologies Conference.2011.DOI:10.2514/6.2011-2269.
3. Sziroczak D , Smith H .A review of design issues specific to hypersonic flight vehicles[J].Progress in Aerospace Sciences, 2016, 84(jul.):1-28.DOI:10.1016/j.paerosci.2016.04.001.
4. Spravka J J , Jorris T R .Current Hypersonic and Space Vehicle Flight Test and Instrumentation[J]. 2015.
5. Magee T, Fugal S, Fink L, et al. Boeing N+ 2 supersonic experimental validation phase II program[C]//32nd AIAA Applied Aerodynamics Conference. 2014: 2137.
6. Bing X ,XiaoQiang F ,Yi W .Deficiencies of streamline tracing techniques for designing hypersonic inlets and potential solutions[J].Science China(Technological Sciences),2020,63(03):488-495.
7. Mölder S.Internal,axisymmetric,conical flow [J] .AIAA Journal,1967,5(7):1252-1255.
8. Molder S,Szpiro E J. Busemann Inlet for Hypersonic Speeds[J]. Journal of Spacecraft and Rockets,1966,3(8):1303-1304.
9. Guo J, Huang G. Study of Internal Compression Flowfield for Improving the Outflow Uniformity of Internal Waverider[J]. Journal of Astronautics,2009,30(05)

10. Musa, Omer;Guoping Huang;Bo Jin;Mölder, Sannu;Zonghan Yu.New Parent Flowfield for Streamline-Traced Intakes.[J].AIAA Journal,2023,Vol.61(7): 2906-2921
11. Zhang K .Hypersonic Curved Compression Inlet and Its Inverse Design[J]. 2020.DOI:10.1007/978-981-15-0727-4.
12. Fang X, Zhang K Y. Inverse design of supersonic internal flow path based on given outflow velocity profile[C]//48th AIAA/ASME/SAE/ASEE Joint Propulsion Conference & Exhibit. 2012: 4064.
13. Zhou H, ** Z, Zhuang G, et al. Space-streamline-based method of characteristics for inverse design of three-dimensional super/hypersonic flows[J]. Physics of Fluids, 2022, 34(8).
14. Qiao W, Yu A, Wang Y. An Inverse Design Method for Non-uniform Flow Inlet with a Given Shock Wave[J]. Acta Mathematicae Applicatae Sinica, English Series, 2019, 35(2): 287-304.
15. Wang J, Cai J, Duan Y, et al. Design of shape morphing hypersonic inward-turning inlet using multistage optimization[J]. Aerospace Science and Technology, 2017, 66: 44-58.
16. Yue Ma, Mingming Guo, Yi Zhang, Jialing Le, Ye Tian, Shuhong Tong, Hua Zhang, Fei Tang, Zeyang Zhao; Dynamic multi-objective optimization of scramjet inlet based on small-sample Kriging model. Physics of Fluids 1 September 2023; 35 (9): 095136.
17. Damm K A , Gollan R J , Jacobs P A ,et al.Discrete Adjoint Optimization of a Hypersonic Inlet[J].AIAA Journal, 2020, 58(6):1-14.DOI:10.2514/1.J058913.
18. Wenyou,QIAO,Anyuan,et al.Design method with controllable velocity direction at throat for inward-turning inlets[J].Chinese Journal of Aeronautics, 2019, v.32;No.159(06):55-67.DOI:10.1016/j.cja.2019.04.012.
19. Hohn O M ,Ali Gülhan.Experimental Investigation of Sidewall Compression and Internal Contraction in a Scramjet Inlet[J].Journal of propulsion and power, 2017, 33(2):501-513.DOI:10.2514/1.b36054.
20. McClinton C R.High speed/hypersonic aircraft propulsion technology development［A］.//Advances on Propulsion Technology for High-Speed Aircraft,AVT-150 RTO AVT/VKI Lecture Series［C］.Rhode St.Genese,2007
21. Bolender M, Wilkin H, Jacobsen L, et al. Flight dynamics of a hypersonic vehicle during inlet un-start[C]//16th AIAA/DLR/DGLR International Space Planes and Hypersonic Systems and Technologies Conference. 2009: 7292.
22. Ferrero A. Control of a supersonic inlet in off-design conditions with plasma actuators and bleed[J]. Aerospace, 2020, 7(3): 32.
23. Smart M K. How much compression should a scramjet inlet do?[J]. AIAA journal, 2012, 50(3): 610-619.
24. John W. Slater, Arjun J. Vedam, William Engblom, and Jacob Snider, "Numerical Evaluation of Hypersonic Inward-Turning Inlets at Off-Design Mach Number." American Institute of Aeronautics and Astronautics.
25. WANG X F, QU F, FU J J, et al. Discretized adjoint based aerodynamic design optimization for the hypersonic inward turning inlet[J]. Acta Aeronautica et Astronautica Sinica, 2023, 44: 128352 (in Chinese). doi: 10.7527/S1000-6893.2023.28352
26. Brahmachary, S., Fujio, C., Aksay, M., and Ogawa, H., "Design optimization and off-design performance analysis of axisymmetric scramjet intakes for ascent flight", Physics of Fluids, vol. 34, no. 3, 2022. doi:10.1063/5.0080272.
27. Fujio C, Ogawa H. Physical insights into multi-point global optimum design of scramjet intakes for ascent flight[J]. Acta Astronautica, 2022, 194: 59-75.
28. Ogawa H, Boyce R R. Physical insight into scramjet inlet behavior via multi-objective design optimization[J]. AIAA journal, 2012, 50(8): 1773-1783.

29. Fujio C, Ogawa H. Scramjet Intake Design Based on Exit Flow Profile via Global Optimization and Deep Learning toward Inverse Design[C]//AIAA SCITECH 2022 Forum. 2022: 1408.
30. Reinartz B U, Herrmann C D, Ballmann J, et al. Aerodynamic performance analysis of a hypersonic inlet isolator using computation and experiment[J]. Journal of Propulsion and Power, 2003, 19(5): 868-875.